David Weyers; Akash Mistry; Krzystof Nieweglowski; Karlheinz Bock

Hybrid lithography approach for single mode polymeric waveguides and out-of-plane coupling mirrors

Erstveröffentlichung in / First published in:

Electronic Components and Technology Conference (ECTC). San Diego, 31.05.-03.06.2022. IEEE, S. 1919 - 1926. ISBN 978-1-6654-7943-1.

DOI: https://doi.org/10.1109/ECTC51906.2022.00301

Final edited form was published in "Electronic Components and Technology Conference (ECTC). San Diego 2022", S. 1919 - 1926, ISBN 978-1-6654-7943-1
https://doi.org/10.1109/ECTC51906.2022.00301

Hybrid lithography approach for single mode polymeric waveguides and out-of-plane coupling mirrors

David Weyers, Akash Mistry, Krzystof Nieweglowski and Karlheinz Bock
Institute of Electronic Packaging Technology
Technical University of Dresden, D-01062 Dresden, Germany
Email: david.weyers@tu-dresden.de

***Abstract*—This paper describes technology and process development for a hybrid lithography approach pairing UV-lithography for planar single mode waveguides with 2-photon-polymerization direct-laser-writing for out-of-plane coupling mirrors. Improvements to multi-layer direct patterning of OrmoCore/-Clad material system using UV-lithography are presented. Near square core cross sections are achieved. Minimum alignment accuracy at $\approx 3\,\mu m$ is observed. Cut-back measurement on single mode waveguides shows attenuation of $0.64\,dB\,cm^{-1}$ and $1.5\,dB\,cm^{-1}$ at $1310\,nm$ and $1550\,nm$ respectively . Up to 2.5-times increase of shear-strength after thermal exposure up to $300\,°C$ is found using shear tests and compared for various surface treatments. Mechanical compatibility to reflow soldering is derived. An extensive study on the pattering of ORMOCER® using 2-photon-polymerization is performed. Flat $45°$-micro mirrors with sub-$10\,\mu m$ dimensions are 3D-printed both in OrmoCore and OrmoComp. Outlook to further research on hybrid lithography integration approach is given.**

***Keywords*—optical interconnects, single mode, ORMOCER®, hybrid lithography, direct patterning, UV-lithography, 2-photon-polymerization direct-laser-writing, micro-mirrors**

I. Introduction

The demand for integration of optics in electronics systems given by the ongoing evolution of high performance computing (HPC) in the last decade is now extended by the increasing fabrication volume of integrated photonics on chip-level, mainly Si- and III-V-photonics. In both cases the focus is on single mode waveguiding in the 2nd and 3rd datacom window at $1310\,nm$ and $1550\,nm$, respectively.

Single mode fibers are the dominating optical interconnect for rack-level and above, but can not be integrated dense and parallel enough to contact photonics on chip-level. However, the capability of polymer waveguides (WG) to bridge this gap on interposer and module level has been largely demonstrated [1]–[5]. Yet, the coupling between interposer- and chip-level represents a major challenge due to the large difference in refractive index and numerical aperture (NA) from integrated inorganic to polymer WGs. The three currently available approaches namely fiber grating couplers (FGC), edge and adiabatic coupling all have drawbacks [6]. Edge coupling demands a mode size converter and IO-count is limited by small available area on chip edge, adiabatic coupling suffers from long transition length and direct contact between both WGs needed [4], [5] and vertical coupling using FGC has low bandwidth and needs a micro-mirror to couple the vertical beam into planar polymer WGs [1], [2]. FGCs allow for wafer level probing and ease testing for R&D stage. In addition, current applications use a narrow optical bandwidth, thus FGCs are mainly used for integrated photonics and consequently also the coupling approach we focus on.

A. Hybrid Lithography

In [7] the ability of 2-photon-polymerization direct-laser-writing (2PP-DLW) to structure free form lenses and total-internal-reflection (TIR) mirrors for coupling between single mode WGs has been shown. In [8] we scaled down direct UV-lithographic structuring of ORMOCER®based polymer WGs from multi to single mode We propose a combination of these two as a hybrid lithography approach to manufacture a planar optical RDL including mirrors based on TIR coupling to FGCs and other vertical emitters and receivers, such as VCSELs and photodiodes.

Fig. 1 schematically shows an interconnect made using the hybrid lithography approach. Wafer-scale UV-lithography is used to directly pattern lower and upper clad and the structured WGs in the core layer, forming an optical RDL in a parallel, high throughput process. Openings for the coupling mirrors are structured in the full stack or at least in core and upper clad. Micro-mirrors are then formed in ORMOCER®using 2PP-DLW process, allowing for arbitrary three dimensional shapes of the micro-mirrors.

Since the process is mask-less and serial, shape and position of the mirrors can be adapted quickly and allows for rapid-

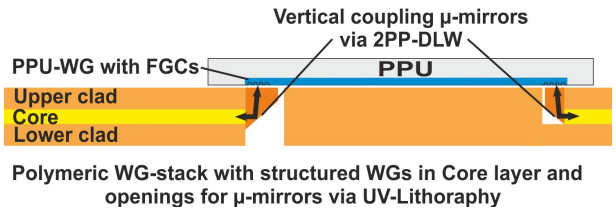

Fig. 1. Schematic of polymeric RDL with vertical coupling micro-mirrors made with the hybrid lithography approach connected to a PPU with integrated WGs and FGCs.

Final edited form was published in "Electronic Components and Technology Conference (ECTC). San Diego 2022", S. 1919 - 1926, ISBN 978-1-6654-7943-1
https://doi.org/10.1109/ECTC51906.2022.00301

prototyping. However processing time is directly depending on polymerized volume. In order to keep a feasible processing time, we limit the use of this process to the micro-mirrors, where it's strength can be fully utilized.

B. Silhouette Platform

The Silhouette project aims to develop a platform for the co-integration of novel photonic processing units (PPU) utilizing optical effects for encryption with ASICs and discrete devices such as laser- and photo diodes on an electro-optical (E/O) interposer. Alignment and assembly of E/O components pose as the main challenge for such systems, especially if the IO-count is high. By co-designing and manufacturing all components within the project consortium these can be efficiently addressed and process compatibility can be assured.
Fig. 2 schematically pictures the aimed integration approach. The described polymeric RDL is added to a conventional silicon interposer with electrical copper RDL and assembly pads as a back end of line (BEOL) layer supply optical function and form the E/O interposer. Micro-mirrors realize the optical interconnect to chip-level and edge coupling to single fibers or fiber arrays is used for external optical connections. Pad spaces are uncovered by the polymer so that during assembly interconnect to devices is simultaneously acting as a through-polymer-via through the $35\,\mu\mathrm{m}$ thick polymer stack. This consists of $7\,\mu\mathrm{m}$ thick core-layer, with cladding twice its thickness to both sides. Simulations in [8] show, that thinner clad might lead to excess loss due to the weak guiding WGs with significant power transmission through clad.

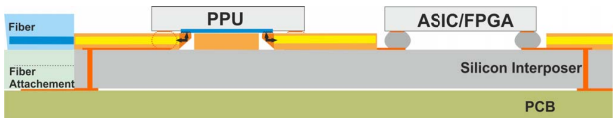

Fig. 2. Integration approach of the Silhouette project forming a E/O interposer by adding the optical RDL as a BEOL-layer onto a silicon interposer with electrical RDL and Pads for electrical interconnects.

To implement this approach we first address issues with repeatability of UV-lithography reported in [8] in section II and manufacture straight planar WGs. The process is then refined for subsequent patterning of three polymer layers. Pillars for shear-testing are manufactured using different surface preparation and adhesion promoters.
Produced WGs are then optically characterized and attenuation is derived from cut-back measurement in section III. Facet preparation via dicing and breaking after cleacing via dicing or laser-cutting are compared.
In section IV we expose these samples to temperatures up to $300\,^{\circ}\mathrm{C}$ and conduct shear-testing to show compatibility to reflow soldering and identify best surface preparation.
Hybrid lithography approach is completed in section V with extensive study of patterning ORMOCER®-materials OrmoCore and OrmoComp using 2PP-DLW. Initial tests on fused silica substrates with low reflection show feasibility of both materials with OrmoComp beeing more suited. Transition to silicon substrates introduces reflection effects and standing wave patterns, that can be bypassed by lifting the mirrors on a base or writing on top of bottom clad layer. Smooth $45\,\mathrm{deg}$-micro-mirrors are printed with both materials.
Finally, we conclude our results and discuss further research goals.

II. UV-Lithography

In [8] we improved our UV-lithographic direct patterning of WGs from multi to single mode dimensions. Simulations showed best mode matching to common single mode fibers and FGCs for NA of 0.14 and square cross section between $6\,\mu\mathrm{m}$ and $7\,\mu\mathrm{m}$. Best results were achieved for an exposure time of $0.15\,\mathrm{s}$ using an Hg-lamp with 16 to $18\,\mathrm{mW\,cm^{-2}}$, corresponding to a dose of $\approx 2.55\,\mathrm{mJ\,cm^{-2}}$. Repeatability however was difficult with these settings.
First, we measured the uniformity of UV-light power density PD across 9 points on a 6" wafer defined as $(PD_{\max} - PD_{\min})/(PD_{\max} + PD_{\min})$ to $3.5\,\%$ using a Thorlabs PM100D power meter with S120VC diode set to $365\,\mathrm{nm}$. By replacing and adjusting the lamp we improved that value to $2\,\%$. Dose measurement for $0.15\,\mathrm{s}$ exposure time resulted in a deviation of $\pm 10\,\%$ for 10 exposures. We concluded that the shutter is reliable for such low exposure times. Further measurements revealed that $\geq 1\,\mathrm{s}$ to decrease the deviation below $\pm 1\,\%$. Intensity had to be adapted to $\approx 5.5\,\mathrm{mW\,cm^{-2}}$ by reducing the lamp power and increasing distance between lamp and wafer to remain with the same dose.

A. Multi-layer WG-Stack

In [8] we manufactured WGs with a structured core in full bottom and top clad. WG-stack build-up process flow and development is described in detail.
Continuing these works we first manufactured straight WGs for cut-back measurement with unstructured clad according to the slightly altered version in tab. I. By better control over dose we achieved nearly square cross section in fig. 3b, however sidewalls are still rough and cross section varies across wafer due to inhomogeneous UV-intensity. This is visible in comparison between fig. 3a and 3b.

For the hybrid lithography approach all three polymer layers have to be patterned, precise overlay accuracy is needed, ideally below $1\,\mu\mathrm{m}$. OrmoCore and -Clad are both highly transparent for visible light and refractive index contrast between clad and core layer is low, making structures in these layers barely visible under microscopes for alignment in UV-lithography and 2PP-DLW tools. Thus, an additional metal layer for alignment of WG-stack globally and micro-mirrors locally was introduced. For initial experiments we used AZ 5214E resists to lift-off pattern a layer of $50\,\mathrm{nm}$ of WTi and $100\,\mathrm{nm}$ of Cu sputtered onto 4" silicon wafers. Later this can be included in the electrical RDL according to fig. 2, which will also be used for PPU self-alignment

Final edited form was published in "Electronic Components and Technology Conference (ECTC). San Diego 2022", S. 1919 - 1926, ISBN 978-1-6654-7943-1
https://doi.org/10.1109/ECTC51906.2022.00301

TABLE I
PROCESS FLOW FOR ORMOCORE/-CLAD REPEATED THREE TIMES FOR MULTI-LAYER WG-STACK

1. Resist preparation	Mix by weight ratio, stir 2 h, degas 5 min @ 200 mPa
2. Clean (only Si)	Acetone/IPA/DI-Water spin-clean
3. Surface activation	O_2-Plasma 5 min Si/ 3 min ORMOCER®
4. Reference wafer	4-point contact wafer against mask
5. Spin-coating	Pipette defined volume to center, 30 s @ target RPM, edge beat removal (EBR): spray OrmoThin on edge for last 10 s
6. Soft bake	4 min @ 85 °C on hotplate with N_2-flow
7. Exposure	2 min N_2-flow with 100 µm separation, Alignment with 10 µm separation, Exposure with 1 µm proximity gap
8. Post exposure bake	10 min @ 130 °C on hotplate with N_2-flow
9. Puddle development	30 s each with OrmoDev and IPA, IPA rinse, N_2-blow dry
10. Full exposure	300 s
11. Hard bake full stack	3 h @ 150 °C with 5 K min^{-1} ramp

between solder-bumps and pads during reflow process. By referencing all subsequent layers to the metal layer minimal missalignment in the optical interconnect formed via the polymer WG, TIR-micro-mirror and FGC to on-chip WG is ensured.

Process flow according to Tab. I is repeated to form the three layers. Diluted resists are needed to spin-coat thin layers. This also eases stirring, allows for degassing in vacuum and application of defined volumes with pipettes, both alleviating problems with layer homogeneity we previously reported. We use OrmoCore diluted 4:1 with OrmoThin for the WG core and a mixture of 70 % OrmoCore and 30 % OrmoClad diluted 2:1 with OrmoThin as clad. OrmoCore/-Clad mixture ratio gives the desired NA of 0.14 [9]. Resists mixtures are prepared just before application to ensure homogeneity. Surface preparation measures will be described and compared later. In [8] we explained the need for a thin proximity gap, thus each wafer is referenced against the mask before applying the resist and EBR is performed during spin-coating. For bottom clad we use 4 mL spun at 1000 RPM, for core 3 mL at 3000 RPM and for top clad 5 mL spun at 1000 RPM. Top clad resist is applied to the entire surface with the pipette, otherwise WG cores will deflect resin during spin coating and leave shadowed areas uncoated.

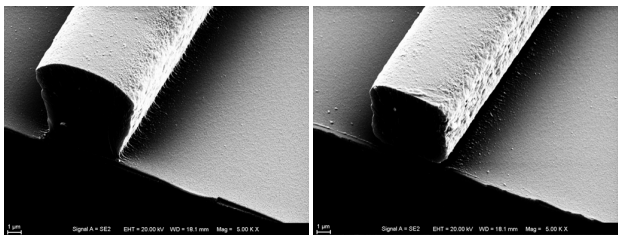

(a) (b)

Fig. 3. Best achieved cross-sections for 7 µm mask opening. Varying UV-intensity leads to different cross sections across same wafer in (a) and (b). Slight underexposure leads to concave shape in (a), near square shape is achieved in (a). Rough sidewalls are visible for both.

Exposure time has to be adapted according to layout and layer thickness. OrmoCore and -Clad are negative tone resist, mask for clad is nearly fully open with only small opaque squares forming mirror and pad openings. In contrast, core layer mask is nearly fully opaque with open 7 µm lines forming the WGs. Thus, even though 14 µm clad is twice the thickness of 7 µm core, overexposure reduces opening size. Consequently, exposure time had to be set so that the dose is just barely above dose to size of an unstructured layer. We halved UV-intensity again to $\approx 2.75\,mW\,cm^{-2}$ to remain within reliable shutter operation. Best results were achieved for 1 s, same as for half as thick core-layer at double intensity. Fig. 4 shows structured bottom clad with WG-core on top and quantifies misalignment of $\approx$ 3 µm. To improve alignment, vision system in mask aligner had to be complemented with 50x optics in addition to the existing 10x optics, so that the smallest fiducials in mask and metal layer with a line width of 3.2 µm could be aligned. However, it was observed that the stage drifts after alignment, resulting in critical offset for single mode optical structures.

Fig. 4 additionally shows rounding of the square opening and ending of core strip due to proximity effect. Both are acceptable since feature size in mask can be adjusted to give enough space for the mirror and refraction at the interface from WG-end towards clad should be negligible due to small refractive index step. In addition, core is recessed from mirror opening by 2 µm in masks, so that the patterns don't overlap. Even with misalignment, the core will not extend into the opening and patterning quality will not be impeded by structuring on previous topography.

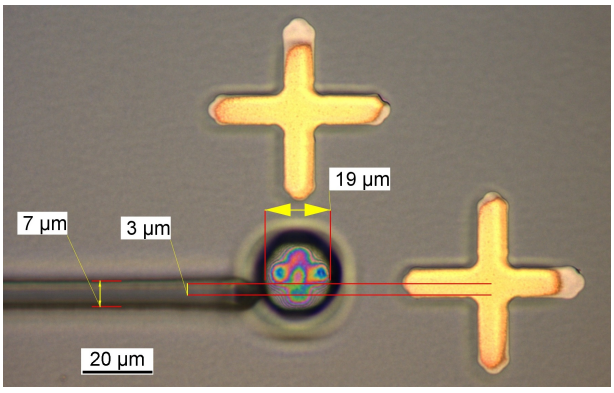

Fig. 4. Bottom clad with 19 µm opening, 7 µm WG in core and metal crosses for mirror alignment. Misalignment is measured at $\approx$ 3 µm

Samples for temperature exposure tests with pillars were structured both in clad directly on silicon and in core on clad. We tested different surface preparations: All wafers were cleaned according to step 2. As silicon surface treatments we compared O_2-plasma (200 W for 5 min), which was previously

Final edited form was published in "Electronic Components and Technology Conference (ECTC). San Diego 2022", S. 1919 - 1926, ISBN 978-1-6654-7943-1
https://doi.org/10.1109/ECTC51906.2022.00301

used, dehydration bake ($5\,\mathrm{min}$ at $200\,^{\circ}\mathrm{C}$), no treatment and OrmoPrime adhesion promoter. For this the wafer was first exposed to $200\,\mathrm{W}$ O_2-plasma for $5\,\mathrm{min}$, then $1.5\,\mathrm{mL}$ of OrmoPrime were dispensed and coated at $4000\,\mathrm{RPM}$ for $1\,\mathrm{min}$. Finally, the sample was then at baked $150\,^{\circ}\mathrm{C}$ for $5\,\mathrm{min}$. Mixture of $70\,\%$ OrmoCore and 30% was coated at $2000\,\mathrm{RPM}$ on all wafers to achieve $40\,\mu\mathrm{m}$ thickness. A homogeneous layer was formed on all samples, only scratches in the OrmoPrime layer were not covered by the resist. Process flow from tab. 1 was used to finish the samples. Exposure time of $3\,\mathrm{s}$ was derived from previous tests and yielded good patterning result with small meniscus.

For adhesion between ORMOCER®-layers a full clad $40\,\mu\mathrm{m}$ was first applied to silicon according to tab. I. Wafers were then exposed to either $3\,\mathrm{min}$ $200\,\mathrm{W}$ O_2-plasma, $5\,\mathrm{min}$ dehydration at $200\,^{\circ}\mathrm{C}$ or no pretreatment. OrmoCore was spin-coated at $2000\,\mathrm{RPM}$ to achieve $40\,\mu\mathrm{m}$ layer thickness. During soft bake however the uniform layer would dewet and form droplets on the samples that were baked or not pretreated. We concluded that surface activation with O_2-plasma is necessary when coating OrmoCore- and Clad on each other. Only this sample was finished following tab. I. Since exposure was on clad and not highly reflective silicon time was increased to $3.5\,\mathrm{s}$. For $3\,\mathrm{s}$ pillars would not be fully polymerized to the bottom.

III. Optical Characterization

In [8] we reported single mode operation of WGs using a beam profiler and coupling efficiency measurement using cleaved SMF-28®Ultra and FG105LCA Fibers as in- and output to WG. Before performing cut-back measurements methods for cutting and their respective WG-facet quality must be studied. Loss at the facet has to be nearly constant across multiple cuts if attenuation is to be reliably derived from cut-back measurements.

Dicing using a wafer saw is the most straight forward approach and gave good results for multi mode WGs [9]. We used $35\,\mu\mathrm{m}$ thin blades for bare silicon and a high feed rate of $4\,\mathrm{mm\,s^{-1}}$ with $20\,000\,\mathrm{RPM}$ to improve cut quality. Fig. 5a shows that the polymer surface is still being scratched in a regular pattern and silicon particles breaking out along the edge. Apart from the facet, WG-stack is not damaged. Interface between the layers and core cross section are barely visible.

Cleaving and breaking is often used for glass fibers or III-V devices. Since structural integrity of the samples is given by the silicon wafer, it has to be cleaved. Laser dicing from the front side allows to align breakpoint to the structures and introduce interrupts of up to $400\,\mu\mathrm{m}$. WGs remain untouched but still break along the cut line. We used an $532\,\mathrm{nm}$ $10\,\mathrm{ps}$ laser with $1\,\mathrm{MHz}$ pulse rate to cut through the polymer and trenches into silicon along the $\{110\}$-plane. Laser power was set to $0.5\,\mathrm{mW}$ and 1000 passes at $500\,\mathrm{mm\,s^{-1}}$ resulted $150\,\mu\mathrm{m}$ cut depth. Initial test with $35\,\mu\mathrm{m}$ clad on silicon gave promising results shown in fig. 5b. Both polymer and silicon have a very smooth facet with few, maximum $500\,\mathrm{nm}$ big particles. Yet, when cleaving and breaking samples with multi-layer WG-stack cracks starting at bottom to top clad interface are introduced. By reducing interrupt length in laser cleave line they were reduced but not below the extend shown in fig. 5c. Inspection under an optical microscope suggest that

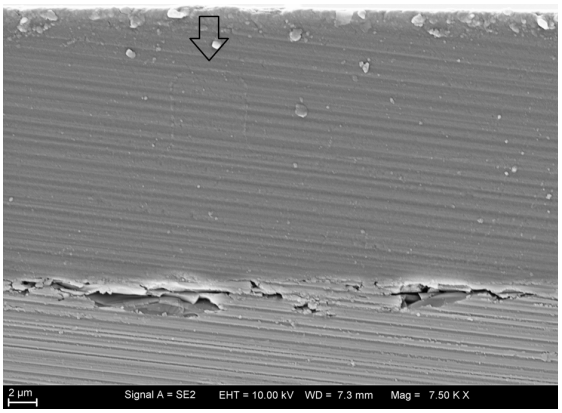

(a)

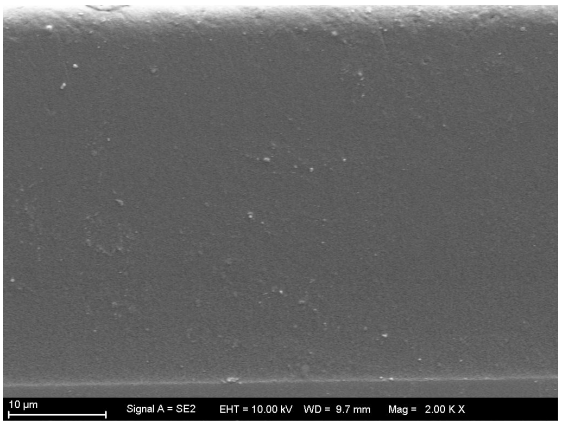

(b)

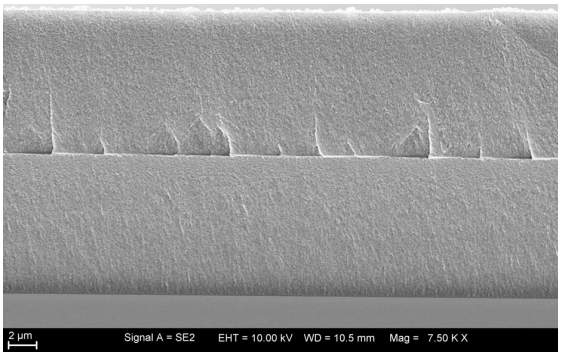

(c)

Fig. 5. SEM-images of facet preparation via dicing in (a), laser cleaving and breaking in (b) and (c). Silicon facet is at the bottom followed by full WG-stack in (a) and (c) and a $35\,\mu\mathrm{m}$ clad layer in (b). Dicing scratches the surfaces and chips silicon along the edge but no signs of cracks in between ORMOCER®-layers or around core visible in (a). Laser cleaving and breaking gives smooth surface for a single ORMOCER®-layer in (b) but cracks in WG-stack between bottom and top clad in (c).

Final edited form was published in "Electronic Components and Technology Conference (ECTC). San Diego 2022", S. 1919 - 1926, ISBN 978-1-6654-7943-1
https://doi.org/10.1109/ECTC51906.2022.00301

they extend laterally into the WG-stack and go along and through core cross-section. High and varying excess loss will be introduced to WGs, thus use of this method for facet definition is impeded.

Additionally we cleaved by cutting $250\,\mu m$ into silicon from the backside and breaking subsequently. Yet, this leads to a very large extend of cracks in WG-stack. Since cutting WGs is only needed for cut-back measurements and facets will else be defined lithographically, no further research was conducted and dicing was used for cut-back measurements.

Five WGs were measured at five different length to counter statistical deviation from facet preparation, which is substantiated by tolerance between data points and regression line in fig. 6. Least square method was used to derive linear fit and coupling loss of $0.26\,dB$ and $0.38\,dB$, attenuation of $0.64\,dB\,cm^{-1}$ and $1.5\,dB\,cm^{-1}$ at $1310\,nm$ and $1550\,nm$, respectively. Low coupling loss is achieved via mode matching between input single mode fiber and polymeric WG and large output fiber. WG-attenuation is roughly three times higher than material absorption of $0.28\,dB\,cm^{-1}$ and $0.42\,dB\,cm^{-1}$ at $1310\,nm$ and $1550\,nm$, respectively [10]. This is caused by roughness and small defects in WGs.

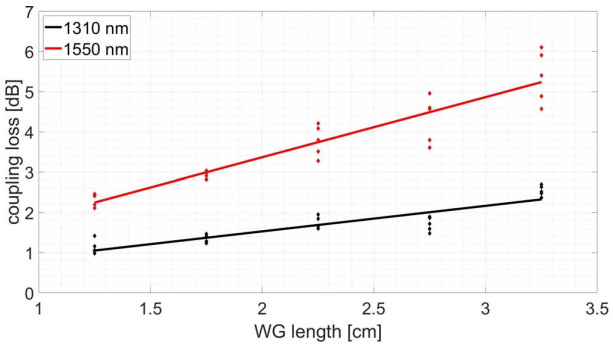

Fig. 6. Loss measurement at $1310\,nm$ and $1550\,nm$ from 5 WGs cut-back from $32.5\,mm$ to $12.5\,mm$ in $5\,mm$ increments. Interpolation gives coupling loss

IV. Temperature Resistance

To characterize thermal stability of WG-stack and compare surface treatments, samples were exposed to temperatures from 250 to $300\,°C$. A hotplate with active temperature control and cooling was used. Fig. 7 shows measured curve, which was chosen similar to typical reflow profiles. Heat-up time is set to $300\,s$ so that gradient is below $1\,K\,s^{-1}$ to prevent stress due to thermal shock. Peak temperature is held for $3\,min$. Cool down takes up to $30\,min$ since cooling gradient is limited to -0.1 to $-0.2\,K\,s^{-1}$.

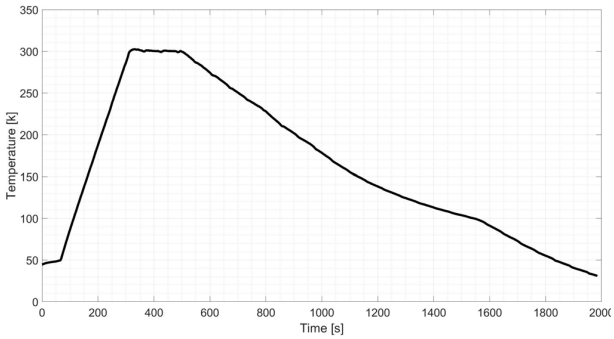

Fig. 7. Temperature profile for peak of $300\,°C$. $300\,s$ heat-up, $180\,s$ at peak and nearly $30\,s$ cool-down due to limited cooling gradient.

For each sample at least 15 pillars were sheared off using a $100\,\mu m$ chisel to characterize shear strength, results are given in fig. 8. For clad on silicon all pillars sheared off-completely, only leaving small residues from the outside meniscus. For core on clad, clad layer was ruptured and sheared off at the interface to silicon. Thus adhesion of ORMOCER® to silicon the mechanical weakest point and less stable then ORMOCER® layers and adhesion between them. Untempered samples show shear strength from 15 to $20\,cN$, with bake and O_2-plasma giving best results. Contrary to expectation, adhesion greatly increases with peak temperature up to $290\,°C$,

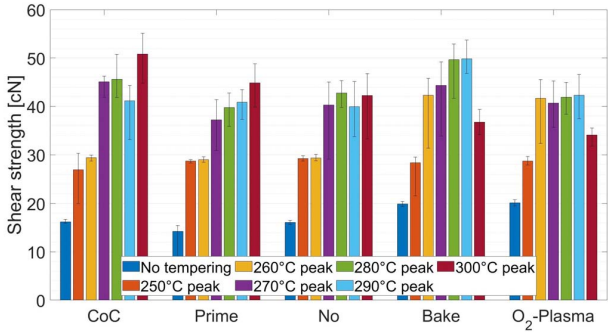

Fig. 8. Shear-strength of core on clad (CoC) with O_2-plasma before both layers and clad on silicon with OrmoPrime, no pretreatment, $5\,min$ at $200\,°C$ and O_2-plasma. Strength is measured without tempering and after exposure to peak temperatures from 250 to $300\,°C$

Final edited form was published in "Electronic Components and Technology Conference (ECTC). San Diego 2022", S. 1919 - 1926, ISBN 978-1-6654-7943-1
https://doi.org/10.1109/ECTC51906.2022.00301

for core on clad, OrmoPrime and no pretreatment even up to $300\,^{\circ}\mathrm{C}$. In all cases, shear strength is higher after temperature exposure, showing compatibility to reflow soldering from mechanical side. Surface pretreatment with OrmoPrime or dehydration for $5\,\mathrm{min}$ at $200\,^{\circ}\mathrm{C}$ give best adhesion after exposure to $300\,^{\circ}\mathrm{C}$. This result might be facility related since OrmoPrime can be applied directly after O_2-plasma activation and resist directly after dehydration on hotplate, whereas a change of labs is necessary between O_2-plasma activation and resist application. This allows for rehydration of the surface and decreases activation. Ideally resist would be applied without exposure to ambient atmosphere after activation.
We conclude that OrmoPrime should be used for best mechanical stability after temperature exposure and that O_2-plasma activation is needed for coating OrmoCore and -Clad on each other.

V. 2-PHOTON-POLYMERIZATION DIRECT-LASER-WRITING

2PP-DLW uses two-photon-absorption (TPA) inside focal point of a highly focused laser beam for additive 3D-structuring of negative tone resists by moving the focal point through resist in a 3D trajectory. Probability of TPA is correlated to intensity square, in contrast to probability of single photon absorption correlating to intensity. This allows the smallest element, so-called volumetric pixel (voxel) to reach resolution below the diffraction limit [11], [12]. Since the laser can be guided in any 3D trajectory, arbitrary shapes can be patterned making this process highly interesting for micro-optical applications.
We used Nanoscribe's Photonic Professional GT2 2PP-DLW-tool, which features a 780 to $800\,\mathrm{nm}$ Ti-sapphire laser with $150\,\mathrm{fs}$ pulses at $76\,\mathrm{MHz}$. Power can be modulated up to $70\,\mathrm{mW}$. 63x magnification lens was used for highest resolution. In-plane beam is guided using a galvanic mirror system before the lens allowing for printing speed from few $\mu\mathrm{m\,s^{-1}}$ to above $100\,\mathrm{mm\,s^{-1}}$. Vertical beam movement of up to $300\,\mu\mathrm{m}$ is given by a piezo stage. Structure is formed by laterally and vertically stacking written lines so that the polymerized volumes overlap. Lateral and vertical line distance are called hatching and slicing, we used $0.1\,\mu\mathrm{m}$ for our structures to achieve low roughness by dense voxel-overlap. Together with laser power and writing speed these are the premier process parameters defining the local dose per volume and thus quality of structure. Mechanical stability and mirror facet precision as well as roughness are the most important characteristics. A process window is defined by the polymerization threshold as lower limit and ability of resist to sustain laser energy as a higher limit. To high energy-input will vaporize resist locally forming gas bubbles that prevent structuring.
OrmoCore shows TPA, but was not designed for 2PP-DLW and is less suitable due to its low sensitivity [13]. Therefore, few results on patterning or OrmoCore via 2PP-DLW have been published [14]–[16]. Nonetheless, we tested OrmoCore for the micro-mirror application due to its excellent optical properties and compatibility to WG-stack in hybrid lithography approach. As a backup we used OrmoComp, which is a highly sensitive resist of the ORMOCER®-family that was designed for 2PP-DLW [13], [17].
To show OrmoCore's capability we first printed on fused silica substrates. Refractive index step to resist is just big enough to reliably reference the interface but reflection is still low, so that it's not affecting structuring quality. The $30\,\mu\mathrm{m}$ long, square $6\,\mu\mathrm{m}$ waveguide with 45°-sloped end facets forming a positive slope micro-mirror in fig. 9 was patterned. High power of $40\,\mathrm{mW}$ with slow $63\,\mu\mathrm{m\,s^{-1}}$ scan speed are necessary due to low sensitivity of OrmoCore.

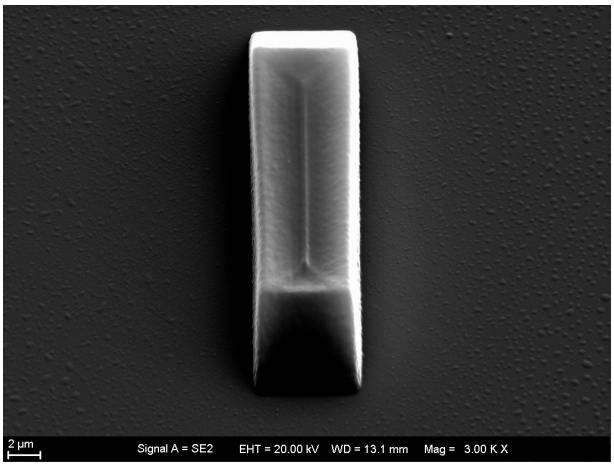

Fig. 9. Best achieved positive slope mirrors in OrmoCore with $30\,\mu\mathrm{m}$ long, square $6\,\mu\mathrm{m}$ connecting WG on fused silica substrate. Hatching and slicing distance is $0.1\,\mu\mathrm{m}$, power and scan speed are $40\,\mathrm{mW}$ and $63\,\mu\mathrm{m\,s^{-1}}$.

We then continued our experiments on silicon, which will be the substrate for E/O-interposer in Silhouette platform. Due to high reflection restricting patterning and forming standing wave patterns we were not able to achieve good results with printing OrmoCore directly on silicon. We attribute this to the small processing window of OrmoCore that we already saw on fused silica. Therefore, we applied $14\,\mu\mathrm{m}$ thick clad layer on-top of silicon using UV-lithography. The high beam divergence greatly reduces reflection intensity in this distance. Interface between clad and liquid OrmoCore can not be detected due to small refractive index step, thus silicon surface is used for reference and structure position is offset by clad thickness. It has to be uniform and well-known for precise alignment.
Fig. 10a shows a $7\,\mu\mathrm{m}$ positive slope micro-mirror in OrmoCore with excellent structuring quality. Surface roughness is superior to what we achieved in section II using UV-lithography and appears to be intrinsic surface roughness of polymer. Corners are a slightly rounded and front mirror edge is shifted to the right. Mirror is formed by overlapping rectangles stacked in each other in-plane, where each rectangle is written as one continuous line. This leads to rounding of corners since laser has finite acceleration

Final edited form was published in "Electronic Components and Technology Conference (ECTC). San Diego 2022", S. 1919 - 1926, ISBN 978-1-6654-7943-1
https://doi.org/10.1109/ECTC51906.2022.00301

when changing direction. Start point of these rectangles is in bottom-right corner, inaccuracy in on-set shifts this point slightly. Thus, the mirror appears concave, but only the front-edge is shifted. Considering these two effects during mirror design, allows to move them away from the actually reflecting surface and prevent effect on optical quality.
Process window of OrmoComp is broader, allowing for printing of an identical structure directly on silicon in shown fig. 10b. Due to higher sensitivity of OrmoComp scan speed is two orders of magnitude bigger with $5000\,\mu\mathrm{m\,s^{-1}}$, greatly reducing printing time compared to OrmoCore. Reflection and standing wave effects are clearly visible on side wall and form a base on the mirror facet. Its roughness is bigger compared to OrmoCore but single printing lines can not be differentiated. Mirror top shows a convex shape that we attribute to overexposure. For such high scan speeds the finite acceleration when changing direction leads to a significantly lower scan speed in corners and consequently higher dose and voxel size compared to straight sections.

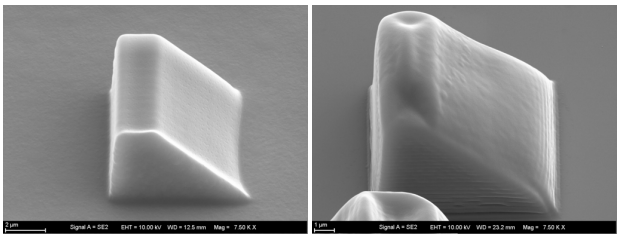

(a) (b)

Fig. 10. Best achieved positive slope mirrors in OrmoCore on clad (a) and OrmoComp on silicon (b). Hatching and slicing distance is $0.1\,\mu\mathrm{m}$ for both, power is $17.5\,\mathrm{mW}$ (a) and $25\,\mathrm{mW}$ (b) and scan speed is $63\,\mu\mathrm{m\,s^{-1}}$ (a) and $5000\,\mu\mathrm{m\,s^{-1}}$.

Finally, we printed a negative slope micro-mirror lifted on a square base out of the reflection affected zone and onto what will be height of WG-core in hybrid lithography approach. As in fig. 1 this allows for the mirror to extend into bottom clad, thus collecting more light and providing higher coupling efficiency compared to printing on clad with OrmoCore. Best achieved result is presented in fig. 11. Decreasing reflection effect with distance to silicon surface is visible at bottom of base. Mirror facet is obscured and quality can not be judged, yet overall structure looks smooth. Nevertheless, this underlines why process development was done for positive slope mirrors and transition to negative slope can only be done after suitable printing parameters are found. By dividing the structure model in to 10 line thick and high contour with fine hatching and slicing of $0.1\,\mu\mathrm{m}$ and a filling with $0.3\,\mu\mathrm{m}$ hatch and slice inside the structure, writing time and overexposure effect were reduced. Yet, flat top of mirror is still slightly concave, which would effect the reflected beam passing through this interface towards the FGC. If this can not be alleviated by changing printing parameters, design has to be adapted.

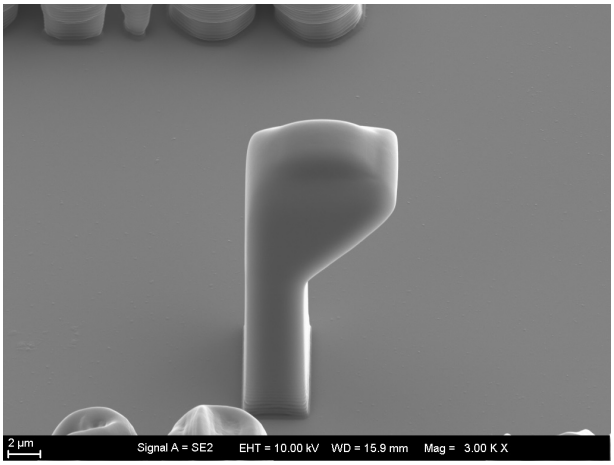

Fig. 11. Best achieved negative slope mirror lifted on base in OrmoComp on silicon. 10 contour lines are written with $0.1\,\mu\mathrm{m}$ hatching and slicing, which is increased to $0.3\,\mu\mathrm{m}$ for fill. Power and scan speed are $25\,\mathrm{mW}$ and $1200\,\mu\mathrm{m\,s^{-1}}$, respectively.

VI. Conclusion and Outlook

We presented our hybrid lithography approach providing an optical RDL with vertical coupling elements to FGCs or other surface emitters/receivers and edge coupling to e.g. fibers. This polymeric optical RDL is then included into the E/O-interposer, which is part of the Silhouette-platform and will provide packaging for novel PPUs. We improved our UV-lithographic patterning of OrmoCore/-Clad material system and demonstrated multi-layer WG-stack with planar, straight single mode WGs and opening for integration of coupling elements via 2PP-DLW. Attenuation of $0.64\,\mathrm{dB\,cm^{-1}}$ and $1.5\,\mathrm{dB\,cm^{-1}}$ at $1310\,\mathrm{nm}$ and $1550\,\mathrm{nm}$, respectively was derived from cut-back measurements. Shear tests were used to show positive impact of thermal exposure up to $300\,^{\circ}\mathrm{C}$ and process compatibility to reflow soldering. Process development for patterning of OrmoCore and OrmoComp using 2PP-DLW lead to micro-mirrors with excellent structuring quality and underlines the feasibility of these process and materials for micro-optical coupling elements.

Next step in developing the hybrid lithography approach is clearly demonstrating optical function and proof of concept by forming an fiber to fiber U-link connection via 2 micro-mirrors and a connecting polymer WG. Beam shape measurements on such a setup would be used to predict and improve coupling efficiency to FGCs. Hereafter, both patterning techniques can be further advanced with respect to alignment, attenuation and coupling efficiency. Positioning accuracy with 2PP-DLW-tool will be characterized and then possibilities to reach sub-µm overlay accuracy in every step will be looked upon. In addition, design features that reduce alignment dependent loss will be studied. More complex mirrors that fully utilize capabilities of 2PP-DLW and are co-designed with FGCs represent

Final edited form was published in "Electronic Components and Technology Conference (ECTC). San Diego 2022", S. 1919 - 1926, ISBN 978-1-6654-7943-1
https://doi.org/10.1109/ECTC51906.2022.00301

a promising approach. We will use tactile profilometry to quantify roughness and will adapt processing to yield $< 0.1\lambda$ roughness.

We will study lithographic patterning of vertical facets in clad and proximity effect on WG-end for edge coupling. Beam shape will be characterized and design eventually adapted to match respective coupling partners. More complex elements such as bends, crossings and tapers will be patterned and analyzed.

Resilience of optical function against temperature exposure will be reviewed to complement results on mechanical resilience in this work.

Aspects related to the integration on to the Silhouette platform's E/O-interposer, such as planarization of copper RDL with the bottom clad layer and impact of underlying electrical lines on WG-attenuation will be studied. Finally, we will integrate, characterize and improve the approach in fig, 2.

ACKNOWLEDGMENT

This Work has been supported by Germany's Federal Ministry of Education and Research (BMBF) within the project VE-Silhouette. The authors would like to thank M. Schaulin, M. Luniak and I. Sotiriou for their contributions

.

REFERENCES

[1] Z. Zhang, D. Felipe, V. Katopodis, P. Groumas, C. Kouloumentas, H. Avramopoulos, J.-Y. Dupuy, A. Konczykowska, A. Dede, A. Beretta, A. Vannucci, G. Cangini, R. Dinu, D. Schmidt, M. Moehrle, P. Runge, J.-H. Choi, H.-G. Bach, N. Grote, N. Keil, and M. Schell, "Hybrid photonic integration on a polymer platform," *Photonics*, vol. 2, no. 3, pp. 1005–1026, 9 2015. [Online]. Available: http://www.mdpi.com/2304-6732/2/3/1005

[2] E. Bosman, G. V. Steenberge, A. Boersma, S. Wiegersma, P. Harmsma, M. Karppinen, T. Korhonen, B. J. Offrein, R. Dangel, A. Daly, M. Ortsiefer, J. Justice, B. Corbett, S. Dorrestein, and J. Duis, "Scalable electro-photonic integration concept based on polymer waveguides," in *Optical Interconnects XVI*, H. Schröder and R. T. Chen, Eds. SPIE, mar 2016.

[3] L. Ma, X. Xu, and Z. He, "Single-mode polymer waveguides and devices for high-speed on-board optical interconnect application," in *Optical Interconnects XIX*, H. Schröder and R. T. Chen, Eds. SPIE, mar 2019.

[4] T. Barwicz, A. Janta-Polczynski, S. Takenobu, K. Watanabe, R. Langlois, Y. Taira, K. Suematsu, H. Numata, B. Peng, S. Kamlapurkar, S. Engelmann, P. Fortier, and N. Boyer, "Advances in interfacing optical fibers to nanophotonic waveguides via mechanically compliant polymer waveguides," *IEEE Journal of Selected Topics in Quantum Electronics*, vol. 26, no. 2, pp. 1–12, mar 2020.

[5] M. Hiltunen, M. T. Harjanne, T. Vehmas, B. Wälchli, P. Heimala, and T. Aalto, "Polymer interposer for efficient light coupling into 3 μm silicon-on-insulator waveguides," in *Optical Interconnects XX*, H. Schröder and R. T. Chen, Eds. SPIE, feb 2020.

[6] R. Marchetti, C. Lacava, L. Carroll, K. Gradkowski, and P. Minzioni, "Coupling strategies for silicon photonics integrated chips [invited]," *Photonics Research*, vol. 7, 01 2019.

[7] P.-I. Dietrich, M. Blaicher, I. Reuter, M. Billah, T. Hoose, A. Hofmann, C. Caer, R. Dangel, B. Offrein, U. Troppenz, M. Moehrle, W. Freude, and C. Koos, "In situ 3d nanoprinting of free-form coupling elements for hybrid photonic integration," *Nature Photonics*, vol. 12, no. 4, pp. 241–247, mar 2018.

[8] D. Weyers, K. Nieweglowski, L. Lorenz, and K. Bock, "Analysis of polymeric singlemode waveguides for inter-system communication," in *2021 23rd European Microelectronics and Packaging Conference & Exhibition (EMPC)*. IEEE, sep 2021.

[9] K. Nieweglowski, R. Rieske, S. Sohr, and K.-J. Wolter, "Design and optimization of planar multimode waveguides for high speed board-level optical interconnects," in *Proc. IEEE 63rd Electronic Components and Technology Conf. (ECTC)*. TU Dresden, 2013, pp. 1898–1904.

[10] F. Kahlenberg and M. Popall, "ORMOCER®s (organic-inorganic hybrid polymers) for telecom applications: Structure/property correlations," *MRS Proceedings*, vol. 847, 2004.

[11] J. Fischer and M. Wegener, "Three-dimensional optical laser lithography beyond the diffraction limit," *Laser & Photonics Reviews*, vol. 7, no. 1, pp. 22–44, mar 2012.

[12] X. Zhou, Y. Hou, and J. Lin, "A review on the processing accuracy of two-photon polymerization," *AIP Advances*, vol. 5, no. 3, p. 030701, mar 2015.

[13] R. Houbertz, G. Domann, J. Schulz, B. Olsowski, L. Fröhlich, and W.-S. Kim, "Impact of photoinitiators on the photopolymerization and the optical properties of inorganic–organic hybrid polymers," *Applied Physics Letters*, vol. 84, no. 7, pp. 1105–1107, feb 2004.

[14] Z. R. Chowdhury and R. Fedosejevs, "Sub-micron resolution three dimensional structure writing using two photon absorption process," in *Photonics North 2006*, P. Mathieu, Ed. SPIE, sep 2006.

[15] S. Rekštytė, A. Žukauskas, V. Purlys, Y. Gordienko, and M. Malinauskas, "Direct laser writing of 3d polymer micro/nanostructures on metallic surfaces," *Applied Surface Science*, vol. 270, pp. 382–387, apr 2013.

[16] F. Jipa, M. Zamfirescu, A. Velea, M. Popescu, and R. Dabu, "Femtosecond laser lithography in organic and non-organic materials," in *Updates in Advanced Lithography*. InTech, jul 2013.

[17] A. Schleunitz, J. J. Klein, A. Krupp, B. Stender, R. Houbertz, and G. Gruetzner, "Evaluation of hybrid polymers for high-precision manufacturing of 3d optical interconnects by two-photon absorption lithography," in *Optical Interconnects XVII*, H. Schröder and R. T. Chen, Eds. SPIE, feb 2017.